CrystEngComm

Accepted Manuscript

ROYAL SOCIETY OF CHEMISTRY

www.rsc.org/crystengcomm

Cite this: DOI: 10.1039/c0xx00000x

www.rsc.org/xxxxxx

ARTICLE TYPE

Synthesis, structures and theoretical investigation of three polyoxomolybdate-based compounds: self-assembling, fragment analysis, orbital interaction, and formation mechanism

Yi-Ping Tong,*[a] Guo-Tian Luo,[b] Jin Zhen,[a] You Shen[a] and Wen-Yan Lin[c]

Received (in XXX, XXX) Xth XXXXXXXXX 20XX, Accepted Xth XXXXXXXXX 20XX
DOI: 10.1039/b000000x

Three Mo_8- and Mo_{12}-based polyoxoanion compounds (1–3), contain $[Mo_8O_{26}]^{4-}$ and $[(SiO_4)(Mo_{12}O_{36})]^{4-}$ anions, have been successfully synthesized by one-pot hydrothermal method, and characterized structurally by X-ray crystallographic method. 1, $[Cu(L')_4]_2[Mo_8O_{26}]$ (L' = 1-methyl-imidazole), contains rarely observed Mo_8-based oblate shell $[Mo_8O_{26}]^{4-}$ polyoxoanion, while 2, $[L"H]_4[SiMo_{12}O_{40}]\cdot 5[L"]\cdot 5H_2O$ (L" = benzotriazole) and 3, $[L"H]_4[SiMo_{12}O_{40}]\cdot 2H_2O$, Mo_{12}-based spherical shell α-Keggin $[(SiO_4)(Mo_{12}O_{36})]^{4-}$ polyoxoanions. Very interested, SiO_4^{4-} fragment is disordered in 2 and that in 3 is ordered. The observation that 1–3 are different in polyoxoanion structures and crystallized in order in the same solution system is very rare so far for POM synthetic chemistry and very interesting for understanding the formation mechanism and self-assembling process of Mo-based polyoxoanions. The fragment analysis based on the clathrate structural model, i.e. $[Mo_8O_{26}]^{4-}$ anion modeled as $[MoO_4]_2^{4-}@Mo_6O_{18}$, and $[(SiO_4)(Mo_{12}O_{36})]^{4-}$ anion modeled as $[SiO_4]^{4-}@[Mo_{12}O_{36}]$ and/or $[SiO_4]^{4-}@[Mo_3O_9]_2@[Mo_6O_{18}]$, and orbital interaction analysis based on extended Hückel theory calculation have been successfully employed to account for the formation mechanism and self-assembling process of fragments and two Mo-based polyoxoanions in 1–3. The calculated large charge transfer and/or high electronic polarization item between fragments provide electronic structural information of structural stability and interpret the fragment-fragment self-assembling process.

Polyoxometalate (POM) chemistry has been in existence for more than a century and still attracts much attention due to their potential applications in catalysis, medicine, magnetism, optics, conductivity, and so forth.[1-4] Polyoxometalate-based compounds are regarded as one of the most promising materials potentially.[5,6] However, how to design and assemble the POM materials with desired structures and functions remains a great challenge. One of the important reasons is that, in addition to the external chemical stimuli, the formation mechanism and self-assembling of different POM topological structures also plays a key role in the assembly process.[7-10]

As being well-known, the basic parent structures (topology) for POM compounds are diversified, including following anion structures, Keggin series, Dawson series, Silverton series, Waugh series, Lindqvist series and Anderson series.[11] The most typical and important topology is the M_{12}-based POM, which has the highest formation tendency in POM compounds, and therefore is particularly worth considering. These M_{12}-based POM topology is $[(XO_4)(M_{12}O_{36})]$-based Keggin series (α-, β-, γ-, δ- and ε-type).[11a] Obviously the α-Keggin is the most important, though it has been investigated for decades.[12,13]

In this work, we focus on the one-pot synthesis, structures and theoretical analyses of three polyoxomolybdate-based compounds,[14,15] $[Cu(L')_4]_2[Mo_8O_{26}]$ (**1**, $C_{32}H_{48}Cu_2Mo_8N_{16}O_{26}$, L' = 1-methyl-imidazole, Scheme 1), $[L"H]_4[SiMo_{12}O_{40}]\cdot 5[L"]\cdot 5H_2O$ (**2**, $C_{54}H_{59}Mo_{12}N_{27}O_{45}Si$, L" = benzotriazole, Scheme 1), and $[L"H]_4[SiMo_{12}O_{40}]\cdot 2H_2O$ (**3**, $C_{24}H_{28}Mo_{12}N_{12}O_{42}Si$), together with clathrate structural model discussion[16] and extended Hückel theory calculation[17] for self-assembling, fragment analysis, orbital interaction, and formation mechanism. Owing to the fact that **1**–**3** are diversified in polyoxoanion structures and therefore is rarely observed in the same one-pot solution system so far for POM synthetic chemistry. Thus this provides special chance for looking into the formation mechanism and self-assembling process of Mo-based polyoxoanions.

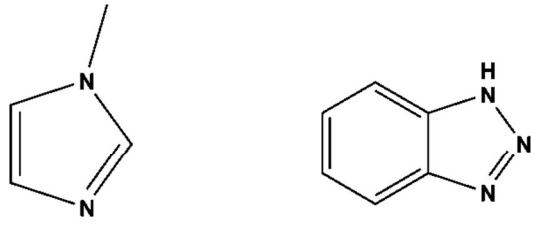

L': 1-methyl-imidazole **L": benzotriazole**

Scheme 1 Organic ligand structures.

Among the three compounds, **1** is a rarely observed Mo_8-based polyoxomolybdate compound of $[Mo_8O_{26}]^{4-}$ polyoxoanion structure, while **2** and **3** are all Mo_{12}-based $[(SiO_4)(Mo_{12}O_{36})]^{4-}$-type ($\alpha$-Keggin) polyoxoanion compopunds.[11a] However, the α-Keggin polyoxoanion in **2** is crystallographicly different from that of **3**, as the four O atoms of SiO_4^{4-} in **2** are disordered over

eight positions, while that in **3** are ordered.

Compounds **1**–**3** were obtained by one-pot hydrothermal reaction of CuO, H_2MoO_4 and hydrofluoric acid with L' and L'' ligands,[14] and characterized crystallographicly (Table S1 in the Supporting Information).[15] The resulting solution was filtrated and kept to unchanged for a few weeks in room temperature for slow vaporization. Very interestingly, **1**–**3** were crystallized from the same solution in order (**1** first, then **2**, and **3** last), which imply that the polymerization process of Mo into polyoxoanions should form similar intermediates (fragments) or building blocks in solution, and further self–assembling of these fragments gives rise to different polyoxoanions.

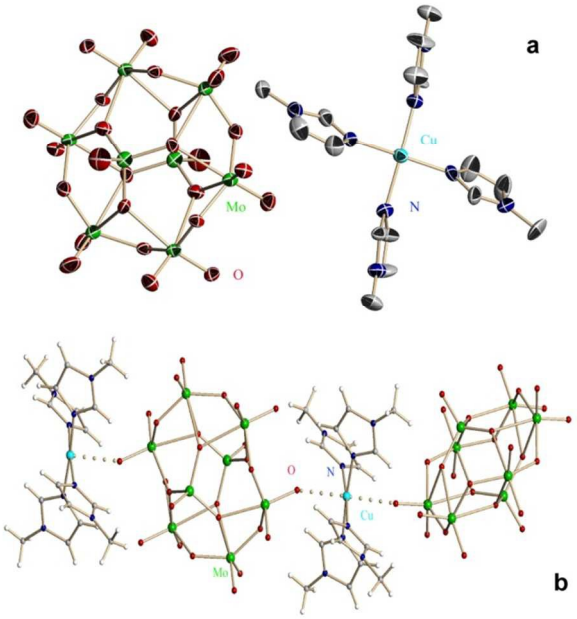

Fig. 1 ORTEP drawing of **1** with 30% thermal ellipsoids (a) and view of a 1D linear chain of **1** (b). The dot line means weak coordinative bonding interaction between $[Cu(L')_4]^{2+}$ and $[Mo_8O_{26}]^{4-}$. Hydrogen atoms are omitted for clarity.

Compound **1** consists of a $[Mo_8O_{26}]^{4-}$ polyoxoanion and two different but symmetrically equivalent Cu(II)-central coordination cations (Fig. 1*a*). Each of the Cu(II) centers lies in a distorted square geometry and is coordinated by four nitrogen atoms from the L' ligands. The Cu–N bond distances and angles around Cu(II) are 2.005–2.024 Å, and the N–Cu–N angles are 92.3(4)–176.0(4)° (Table S2 in Supporting Information). In the axial direction the Cu(II) centers are also weakly coordinated by two terminal O atoms from adjacent $[Mo_8O_{26}]^{4-}$ anions with Cu–O distances being very long 2.479 Å (Fig. 1*b*). Each $[Mo_8O_{26}]^{4-}$ anionic unit coordinate to two adjacent $[Cu(L')_4]^{2+}$ cations *via* two symmetry-related terminal O atoms, featuring repeating $[Cu(L')_4]^{2+}\cdots[Mo_8O_{26}]^{4-}\cdots[Cu(L')_4]^{2+}$ one-dimensional (1D) chains structure (Fig. 1*b*). The two elongated axial Cu–O linkages are marked and can be easily accounted for by the John–Teller effect of d^9 electron configuration Cu(II).

For the $[Mo_8O_{26}]^{4-}$ anion of **1**, it is oblate shell in shape with a circular ring-shape Mo_6O_{18} fragment or moiety caped by two MoO_4^{2-} fragments or moieties below and above in a centrosymmetric arrangement. Among the eight Mo atoms, six Mo atoms from the Mo_6O_{18} fragment are identical with each other, being arranged in a circular ring-shape, and obviously different from another two Mo atoms of MoO_4^{2-} fragments. In the Mo_6O_{18} fragment, each Mo atom has two terminal O atoms (O_t), and linked to two adjacent Mo atoms *via* two bridging O atoms (μ_2-O_b), featuring repeating $-MoO_{2(t)}-O_{(b)}-MoO_{2(t)}-$ units. While for the MoO_4^{2-} fragment, each MoO_4^{2-} has a terminal O atoms (O_t) and three μ_3- bridging O atoms (μ_3-O_b), which bridge MoO_4^{2-} fragment and Mo_6O_{18} circular ring fragment.

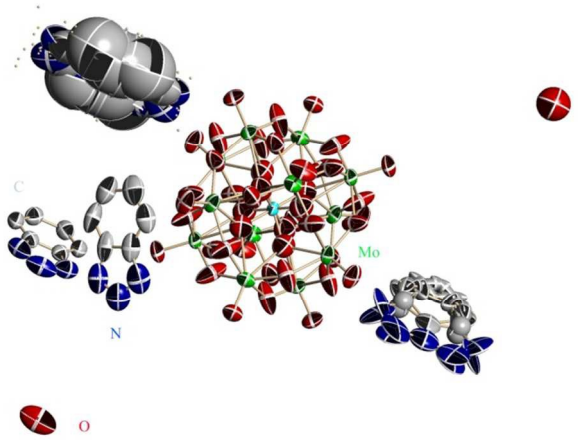

Fig. 2 ORTEP drawing of **2** with 30% thermal ellipsoids. Hydrogen atoms are omitted for clarity.

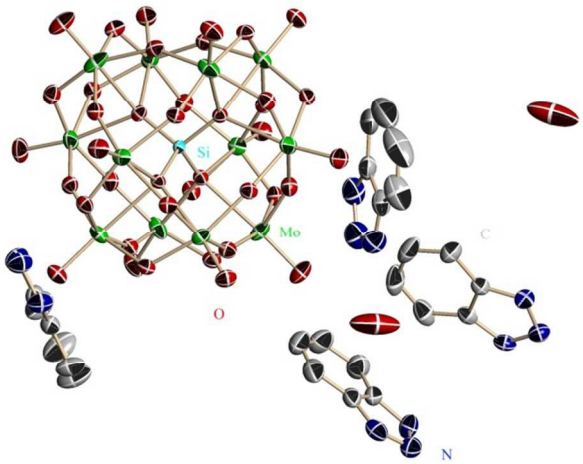

Fig. 3 ORTEP drawing of **3** with 30% thermal ellipsoids. Hydrogen atoms are omitted for clarity.

Compound **2**, i.e. $[L''H]_4[SiMo_{12}O_{40}]\cdot 5[L'']\cdot 5H_2O$, consists of one α-Keggin $[SiMo_{12}O_{40}]^{4-}$ polyoxoanion, four protonated L'' cation ($L''H^+$), five neutral lattice L'' molecules, and five lattice waters (Fig. 2). $L''H^+$ acts as counterion in the crystalline solid. There are very complicated linkages of hydrogen bonding between the four ions/molecules, which link these into rigid solid crystal (Table S3 in the Supporting Information). It is noteworthy that the central SiO_4^{4-} fragment or moiety is disordered over eight O positions, and some $L''H^+$/L'' locate on crystallographic special positions and are highly disordered, thus the treatments for these disordered units are very difficulty, and fortunately the good

quality of the single crystals leads finally to a very satisfactory refinement results with $R_1 = 0.0514$ and $wR_2 = 0.1479$.

For **3**, i.e. $[L''H]_4[SiMo_{12}O_{40}]\cdot 2H_2O$, it consists of one α-Keggin $[SiMo_{12}O_{40}]^{4-}$ polyoxoanion, four protonated L'' cations ($L''H^+$), and two lattice waters (Fig. 3). The $[SiMo_{12}O_{40}]^{4-}$ anion is a

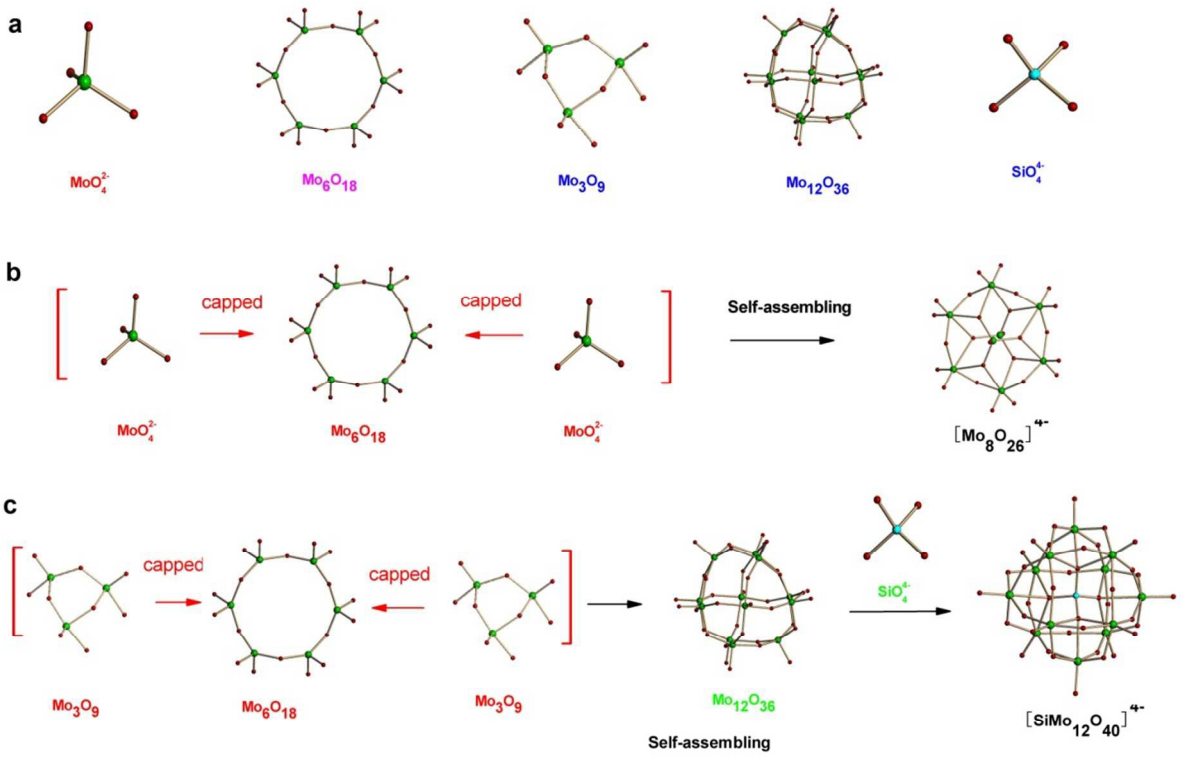

Scheme 2 The fragment constituents of the $[Mo_8O_{26}]^{4-}$ and $[SiMo_{12}O_{40}]^{4-}$ polyoxoanions in **1**–**3** (a), the self-assembling process of fragments of the $[Mo_8O_{26}]^{4-}$ polyoxoanion in **1** (b), and the self-assembling process of fragments of the $[SiMo_{12}O_{40}]^{4-}$ polyoxoanion in **2** and **3** (c).

typical α-Keggin structure, and its SiO_4^{4-} fragment is ordered, which is wholly different from the disordered case in **2**. The $L''H^+$ cation acts as counterion in the crystalline solid, and there are very complicated hydrogen bonding systems between the three ions/molecules, which link these into rigid solid crystal (Table S3 in the Supporting Information).

For the α-Keggin $[SiMo_{12}O_{40}]^{4-}$ polyoxoanion in **2** and **3**, it is a spherical anion in shape, containing a spherical shell ($Mo_{12}O_{36}$ fragment or moiety) and an encapsulated central core (SiO_4^{4-} fragment or moiety). In $Mo_{12}O_{36}$ shell unit, each Mo atom has a terminal O atoms (O_t), and linked to four adjacent Mo atoms *via* four bridging O atoms (μ_2-O_b), thus, twelve Mo atoms are linked into a spherical network, featuring repeating $-O_{(\mu 2\text{-b})}-MoO_{(t)}-O_{(\mu 2\text{-b})}-$ linkages. In SiO_4^{4-} coral fragment, each O atom acts as μ_4-bridging O atom (μ_4-O_b), bridges to three adjacent Mo atoms of the spherical shell, featuring four $Si-O_{(\mu 4\text{-b})}-Mo$ linkages between the SiO_4^{4-} core and $Mo_{12}O_{36}$ shell fragments.

To better understand the structures, formation and self-assembling mechanism, it is necessary to decompose the polyoxoanion clusters in **1**, **2** and **3** into its fragment constituents. For $[Mo_8O_{26}]^{4-}$ anion in **1**, there are, intuitively, two caped MoO_4^{2-} fragments and one ring-shaped Mo_6O_{18} fragment (Scheme 2*a*, 2*b*), thus $[Mo_8O_{26}]^{4-}$ anion can also be presented as $[MoO_4]_2^{4-}@Mo_6O_{18}$ based on the clathrate structural model.[16]

While for $[SiMo_{12}O_{40}]^{4-}$ anion in **2** or **3**, there are an encapsulated SiO_4^{4-} fragment and one shell $Mo_{12}O_{36}$ fragment (Scheme 2*a*), and the shell $Mo_{12}O_{36}$ fragment can be further identified as four trimeric (Mo_3O_9) fragments, which are located in the Si–O bond axial direction of tetrahedral SiO_4^{4-} fragment and bond to the central SiO_4^{4-} fragment *via* μ_4-O_b atoms, or as one ring-shaped Mo_6O_{18} fragment and two caped trimeric (Mo_3O_9) fragments (Scheme 2*c*). Thus the $[SiMo_{12}O_{40}]^{4-}$ anion can also be presented intuitively as $[SiO_4]^{4-}@[Mo_{12}O_{36}]$, or $[SiO_4]^{4-}@[Mo_3O_9]_2@[Mo_6O_{18}]$, or $[SiO_4]^{4-}@[Mo_3O_9]_4$ based on the clathrate structural model. Among the three fragment models, $[SiO_4]^{4-}@[Mo_{12}O_{36}]$ and $[SiO_4]^{4-}@[Mo_3O_9]_2@[Mo_6O_{18}]$ models will be selected for following discussion as they appear to be more acceptable and more intuitive than $[SiO_4]^{4-}@[Mo_3O_9]_4$ model. Moreover in $[SiO_4]^{4-}@[Mo_3O_9]_2@[Mo_6O_{18}]$ model, it contains ring-shaped $[Mo_6O_{18}]$ fragment, and such fragment is also observed in $[Mo_8O_{26}]^{4-}$ anion of **1**, in agreement with the fact that **1**–**3** were crystallized from the same solution, implying that similar intermediates (fragments) or building blocks have been formed in the reaction process. There are also other possible fragment species, but the present fragment decomposition analyses for the two polyoxoanions in **1**–**3** are the most intuitive, and understandable, and should be reasonable and acceptable.

In general, the Mo(VI) and other d^0-metal are polyoxoanion

formers par excellence is clearly due to the fact that they have a favorable combination of ionic radius, charge, and empty *d* orbitals for metal-oxygen π-bonding. Though the full understanding of the formation mechanism and self-assembling processes of the polyoxoanions is still a challenge, as the intermediates or building blocks of the reaction process are hard to measure experimentally and usually presumed theoretically,[18] fragments or moieties of molecules are often related to the intermediates or building blocks of the reaction process. In the present cases, **1–3** were obtained from the same solution system, therefore implying that similar intermediates or building blocks should be formed in the polymerization reaction process and further self-assembling of these intermediates leads to two different polyoxoanions. Here we focus on the fragment decomposition of two obtained polyoxoanions in **1–3**, and deep analysis of fragment orbital interaction of the clathrate structural model based on extended Hückel theory calculation, in order to reveal the self-assembling and formation mechanism of the two polyoxoanion in **1–3**. According to the structural model and the fragment orbital interaction method,[19] the structural stability is ascribed to both charge transfer and the polarization between two fragments. In other words the formation process and stability of two polyoxoanions appear entirely an electronic consequence of the large, highly electron transfer or electronic polarization between fragments.

In the beginning, a MoO_4 or MoO_6 polyhedron can be reasonably assumed based on the knowledge of coordination chemistry, and a followed polymerization process of these MoO_4 or MoO_6 polyhedron units to form polyoxoanion structures can be expected. Then the formations of monomeric MoO_4^{2-} fragment, trimeric Mo_3O_9 fragment, ring-shaped Mo_6O_{18} fragment, spherical shell-shaped $Mo_{12}O_{36}$ fragment, and other fragment species may be quite possible in the polymeric reaction process (Scheme 2*a*). The further self-organizations of these fragment species with each other or other heteratomic species, e.g. SiO_4^{4-}, *etc*., lead to the formation of the final polyoxoanions in **1**–**3**. A diagram for the self-assembling and formation mechanism of these fragments and final polyoxoanions in **1–3** are shown in Scheme 2*b* and 2*c*.

In terms of theoretical calculations of two anions and relative fragments, together with analyses of orbital interactions, charge transfer, electronic polarization of fragments, employed extended Hückel theory method,[17,20] the structures of the two polyoxoanions in **1–3** can be reasonably interpreted. In theory, no charge transfer and no electronic polarization mean no covalent interaction between fragments, and large charge transfer and electronic polarization mean covalent interaction between fragments. For the $[MoO_4]_2^{4-}@Mo_6O_{18}$ fragment model of the $[Mo_8O_{26}]^{4-}$ anion in **1**, the charge donation from two caped monomeric MoO_4^{2-} fragments to a ring-shaped Mo_6O_{18} fragment is 2.38 electrons and electronic polarization in the Mo_6O_{18} fragment is 18.3 orbital% larger than in the two MoO_4^{2-} fragments (Table 1), while for $[SiO_4]^{4-}@[Mo_{12}O_{36}]$ fragment model of the $[SiMo_{12}O_{40}]^{4-}$ anion in **2** and **3**, the calculated charge donation from SiO_4^{4-} fragment to $Mo_{12}O_{36}$ shell fragment is 2.91 electrons and correspondingly a larger electronic polarization occurs in the $Mo_{12}O_{36}$ fragment than in SiO_4^{4-} fragment (33.2 orbital%) (Table 1). The large charge transfer and obvious polarization process observed in both the $[Mo_8O_{26}]^{4-}$ and $[SiMo_{12}O_{40}]^{4-}$ anions accounted for another facts that there are very large interaction energy between the fragments (-888 kcal/mol for the former and -1555 kcal/mol for the latter), and the larger the charge transfer and/or polarization item, the larger the interaction energy. The charge transfer from two MoO_4^{2-} fragments to the Mo_6O_{18} fragment, or the formal charge (4-) of two MoO_4^{2-} fragments delocated over the MoO_4^{2-} and Mo_6O_{18} fragments of the whole $[Mo_8O_{26}]^{4-}$ anion leads a large reorganization of the Mo_6O_{18} fragment. Being similar, the large charge transfer, or the formal charge (4-) of the SiO_4^{4-} fragment delocated over the SiO_4^{4-} fragment and $Mo_{12}O_{36}$ fragments of the whole $[SiMo_{12}O_{40}]^{4-}$ anion leads a large reorganization of the $Mo_{12}O_{36}$ fragment.

Table 1 The calculated charge donation, electronic polarization and interaction energy between fragments of polyoxoanions in **1–3**[a]

	$[Mo_8O_{26}]^{4-}$ in **1**		$[SiMo_{12}O_{40}]^{4-}$ in **2** and **3**	
Net charge donation / electrons	2.38 ($[MoO_4]_2^{4-}$]→Mo_6O_{18})	2.91 (SiO_4^{4-}→$Mo_{12}O_{36}$)	0.11 ($[Mo_3O_9]_2$→Mo_6O_{18})	1.37 (SiO_4^{4-}→Mo_6O_{18})
Electronic polarization / orbital%	18.3 (Mo_6O_{18}–$[MoO_4]_2^{4-}$])	33.2 ($Mo_{12}O_{36}$–SiO_4^{4-})	72.4 (Mo_6O_{18}–$[Mo_3O_9]_2$)	29.1 (Mo_6O_{18}–SiO_4^{4-})
Interaction energy between the fragments / kcal/mol	-888	-1555	-1278	-766

[a] The data is based on G98 calculation.

Somewhat differently for $[SiO_4]^{4-}@[Mo_3O_9]_2@[Mo_6O_{18}]$ fragment model of the $[SiMo_{12}O_{40}]^{4-}$ anion, the calculated charge donation from two caped trimeric (Mo_3O_9) fragment to the ring-shaped Mo_6O_{18} fragment is 0.11 electrons and electronic polarization in Mo_6O_{18} fragment is *ca.* 72.4 orbital% larger than in the $[Mo_3O_9]_2$ fragments. Though the charge transfer is so little (0.11), the high polarization (72.4 orbital%) provides stabilization to the Mo_6O_{18} – $[Mo_3O_9]_2$ fragment assembling process, which is different from the cases of $Mo_{12}O_{36}$ – SiO_4^{4-} fragment assembling process and Mo_6O_{18} – $[MoO_4]_2^{4-}$ fragment assembling process where the charge transfer contributes mainly to the fragment-fragment assembling interaction. The interaction energy for Mo_6O_{18} – $[Mo_3O_9]_2$ fragment assembling process is *ca.* -1278 kcal/mol. Obvious charge transfer from the SiO_4^{4-} fragment to the ring-shaped Mo_6O_{18} fragment (1.37 electrons) and significant electronic polarization of ring-shaped Mo_6O_{18} fragment over the SiO_4^{4-} fragment (29.1 orbital%) have been also observed (Table 1). Fig. 4 shows fragment molecular orbital (MO) interaction of the $[Mo_8O_{26}]^{4-}$ anion. For this anion, all of the 4*d* orbitals of the central Mo(VI) atoms are unoccupied, while the occupied frontier orbitals are all from the oxo orbitals. The LUMO is 4*d* orbital of Mo atoms, and the HOMO is the *p* orbitals of the terminal oxo atoms, which are predominantly from the HOMO-9 (*p* of terminal oxo, 40.3%) and HOMO-13 (*p* of terminal oxo, 24.7%) orbitals

of the Mo_6O_{18} fragment. Owing to orbital interaction of the two MoO_4^{2-} fragments, the HOMO-9 orbital of the Mo_6O_{18} fragment is destabilized, it becomes the HOMO of the $[Mo_8O_{26}]^{4-}$ anion. Differently the HOMO-1 orbital, is an admixture of Mo_6O_{18} fragment orbitals (the HOMO-14, *p* of terminal oxo, 26.5%, and HOMO-3, *p* of terminal oxo, 23.4%) with bridging oxo orbitals (*p*, 12.3%) of two MoO_4^{2-} fragments. However the HOMO-1 and

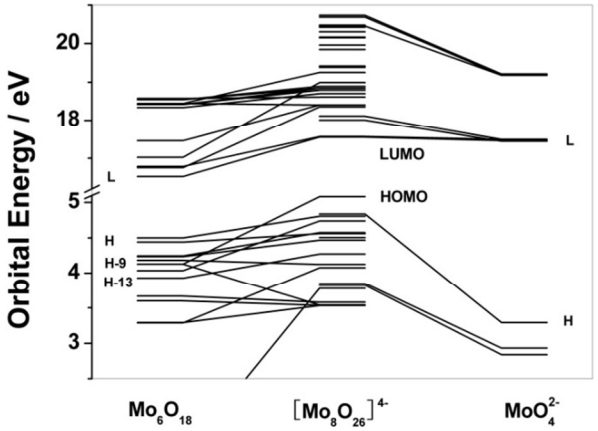

Fig. 4 The fragment orbital interaction diagram of the $[Mo_8O_{26}]^{4-}$ polyoxoanion. H and L represent HOMO and LUMO, respectively.

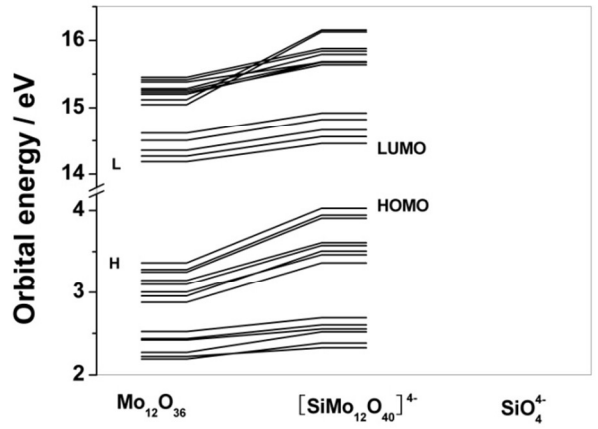

Fig. 5 The fragment orbital interaction diagram of the $[SiMo_{12}O_{40}]^{4-}$ polyoxoanion. H and L represent HOMO and LUMO, respectively.

HOMO are almost degenerate, as both are very closer to each other in energy. Similarly the HOMO-2, HOMO-3 and HOMO-4 are mainly an admixture of *p* of the terminal oxo of the Mo_6O_{18} fragment and *p* of the bridging oxo of the two MoO_4^{2-} fragments. As shown in fragment orbital interaction diagram of $[SiMo_{12}O_{40}]^{4-}$ anion (Fig. 5), the occupied and unoccupied frontier orbitals are all orbitals of the $Mo_{12}O_{36}$ fragment in nature, which are mainly the oxo orbitals, and 4*d* orbitals of Mo(VI) atoms, respectively, and the contribution from SiO_4^{4-} fragment is very little (less than 5%). The HOMO is the HOMO of the $Mo_{12}O_{36}$ fragment, and LUMO is the LUMO of $Mo_{12}O_{36}$ fragment. Owing the orbital interaction of the SiO_4^{4-} fragment, these frontier orbitals of $Mo_{12}O_{36}$ fragment are all wholly destabilized with an obvious increase of energy, and become the frontier orbitals of $[SiMo_{12}O_{40}]^{4-}$ anion. An admixture from bridging oxo orbitals of the SiO_4^{4-} fragment are relatively larger in the occupied orbitals than in the unoccupied orbitals, and thus a relatively larger energy increase can be expected in occupied orbitals than in unoccupied orbitals. For the SiO_4^{4-} fragment since the Si(IV) atom has a tetrahedral geometry, the four sp^3-hybrid Si(IV) orbitals bond to four O atoms (σ-orbitals). These orbitals are doubly occupied, and are formally delocalized over the oxo ligands of the $Mo_{12}O_{36}$ shell fragment. The orbital energies of σ-Si(IV)–O bondings of the SiO_4^{4-} fragment should be shifted to very low values, hence these orbitals will be buried deeply into the occupied oxo orbitals of the $[SiMo_{12}O_{40}]^{4-}$ anion, and are far below the frontier HOMO orbital of the $[SiMo_{12}O_{40}]^{4-}$ anion, an indicative that these bonding interactions are highly stabilized in the $[SiMo_{12}O_{40}]^{4-}$ anion, and that it appears to be a weaker covalent interaction, between the $Mo_{12}O_{36}$ and SiO_4^{4-} fragments in the $[SiMo_{12}O_{40}]^{4-}$ anion, which is in agreement with the experimental observation that SiO_4^{4-} fragment in **2** is disordered.

Conclusions

To summarize, we herein report the one-pot synthesis, structures of three polyoxomolybdate-based compounds (**1**–**3**) containing Mo_8- and Mo_{12}-based polyoxoanions, i.e. $[Mo_8O_{26}]^{4-}$ and $[(SiO_4)(Mo_{12}O_{36})]^{4-}$. **1** contains rarely observed Mo_8-based $[Mo_8O_{26}]^{4-}$ polyoxoanion, while **2** and **3** consist of Mo_{12}-based $[(SiO_4)(Mo_{12}O_{36})]^{4-}$ polyoxoanions. That three compounds are different in the polyoxoanion structures and crystallize in order in the same solution system is very rarely observed so far for POM synthetic chemistry and very interesting for understanding the formation mechanism and self-assembling process of Mo-based polyoxoanions. The fragment analysis and orbital interaction analysis successfully account for the formation mechanism and self-assembling process of fragments and two Mo-based polyoxoanions in **1**–**3**. The calculated large charge transfer and/or high electronic polarization item between fragments provide successfully electronic structural information for interpretation of structural stability and the fragment-fragment self-assembling process.

Acknowledgements

The authors gratefully thank Prof. Xiao-Ming Chen, from School of Chemistry and Chemical Engineering, Sun Yat-Sen University, China, for the invaluable discussion. This work was supported by the National Natural Science Foundation of China (No. 21271080), the Natural Science Foundation of Guangdong Province, China (No. S2012010010311), the General science and technology project on integration of production, education and research, Guangdong Province, China (No. 2012B091100200), the Scientific Foundation of Educational Commission of Guangdong Province, China (No. 2012KJCX0098), and the Science and Technology Planning Project of Huizhou City, Guangdong Province, China (No. 2012B020004006).

Notes and references

[a] Department of Chemical Engineering, Huizhou University, Huizhou 516007, China. Fax: +86-752-2527229; Tel: +86-752-2527229; E-mail: typ2469@163.com
[b] College of Chemistry and Life Science, Gannan Normal University, Ganzhou 341000, China
[c] Department of Life Science, Huizhou University, Huizhou 516007, China

† Electronic Supplementary Information (ESI) available: CCDC reference numbers 985342, 986255 and 771946 for **1**, **2** and **3**, respectively. These data can be obtained free of charge via www.ccdc.cam.ac.uk/conts/retrieving.html (or from the Cambridge Crystallographic Data Centre, 12 Union Road, Cambridge CB21EZ, U.K.; fax (+44) 1223-336-033; or deposit@ccdc.cam.ac.uk). The crystallographic data (Table S1), selected geometric parameters (Table S2), hydrogen bonding linkage (Table S3) and CIF format files for **1**–**3** are available free of charge *via* the Internet at http://pubs.rsc.org. See DOI: 10.1039/b000000x/

1 (a) I. A. Weinstock, E. M. G. Barbuzzi, M. W. Wemple, J. J. Cowan, R. S. Reiner, D. M. Sonnen, R. A. Heintz, J. S. Bond and C. L. Hill, *Nature*, 2001, **414**, 191; (b) I. A. Weinstock, J. J. Cowan, E. M. G. Barbuzzi, H. Zeng and C. L. Hill, *J. Am. Chem. Soc.*, 1999, **121**, 4608.

2 (a) J. J. Cowan, C. L. Hill, R. S. Reiner and I. A. Weinstock, *Inorg. Synth.*, 2002, **33**, 18; (b) J. J. Cowan, A. J. Bailey, R. A. Heintz, B. T. Do, K. I. Hardcastle, C. L. Hill and I. A. Weinstock, *Inorg. Chem.*, 2001, **40**, 6666; (c) L. Chen, D. Shi, J. Zhao, Y. Wang, P. Ma, J. Wang and J. Niu, *Cryst. Growth Des.*, 2011, **11**, 1913; (d) J. Niu, S. Zhang, H. Chen, J. Zhao, P. Ma and J. Wang, *Cryst. Growth Des.*, 2011, **11**, 3769.

3 (a) V. W. Day and W. G. Klemperer, *Science*, 1985, **228**, 533; (b) D. L. Kepert, *Inorg. Chem.*, 1969, **8**, 1556; (c) L. C. W. Baker and J. S. Figgis, *J. Am. Chem. Soc.*, 1970, **92**, 3794.

4 (a) S. Favette, B. Hasenknopf, J. Vaissermann, P. Gouzerh and C. Roux, *Chem. Commun.*, 2003, 2664; (b) M. H. Rosnes, C. Musumeci, C. P. Pradeep, J. S. Mathieson, D.-L. Long, Y.-F. Song, B. Pignataro, R. Cogdell and L. Cronin, *J. Am. Chem. Soc.*, 2010, **132**, 15490.

5 (a) M. T. Pope, *Inorg. Chem.*, 1976, **15**, 2008; (b) M. T. Pope and A.Müller, *Angew. Chem., Int. Ed. Engl.*, 1991, **30**, 34; (c) M. M. Rohmer, M. Bėnard, J.-P. Blaudeau, J. M. Maestre and J. M. Poblet, *Coord. Chem. Rev.*, 1998, **178-180**, 1019.

6 (a) J. M. Maestre, J. M. Poblet, C. Bo, N. Casan-Pastor and P. Gomez-Romero, *Inorg. Chem.*, 1998, **37**, 3444; (b) J. M. Maestre, X. Lopez, C. Bo, J.-M. Poblet and N. Casan-Pastor, *J. Am. Chem. Soc.*, 2001, **123**, 3749; (c) J. M. Maestre, X. Lopez, C. Bo and J. M. Poblet, *Inorg. Chem.*, 2002, **41**, 1883.

7 (a) P. B. Moore, *Neues Jahrb. Mineral. Abb.*, 1974, **120**, 205; (b) H.-J. Lunk, S. Schönherr, *Z. Chem.*, 1987, **27**, 157; (c) H. K. Chae, W. G. Klemperer and V. W. Day, *Inorg. Chem.*, 1989, **28**, 1423.

8 (a) H. Duclusaud and S. A. Borshch, *J. Am. Chem. Soc.*, 2001, **123**, 2825; (b) A. J. Bridgeman and G. Cavigliasso, *Inorg. Chem.*, 2002, **41**, 3500; (c) D. Schaming, C. Allain, R. Farha, M. Goldmann, S. Lobstein, A. Giraudeau, B. Hasenknopf and L. Ruhlmann, *Langmuir.*, 2010, **26**, 5101.

9 (a) Y.-F. Song, D.-L. Long and L. Cronin, *Angew. Chem. Int. Ed.*, 2007, **46**, 3900; (b) Y.-F. Song, N. McMillan, D.-L. Long, S. Kane, J. Malm, M. O. Riehle, C. P. Pradeep, N. Gadegaard and L. Cronin, *J. Am. Chem. Soc.*, 2009, **131**, 1340; (c) J. Zhang, Y.-F. Song, L. Cronin and T. Liu, *J. Am. Chem. Soc.*, 2008, **130**, 14408.

10 (a) M.-H. Zeng, Z. Yin, Y.-X. Tan, W.-X. Zhang, Y.-P. He and M. Kurmoo, *J. Am. Chem. Soc.*, 2014, **136**, 4680; (b) F. Sun, Z. Yin, Q.-Q. Wang, D. Sun and M.-H. Zeng, *Angew. Chem., Int. Ed.*, 2013, **125**, 4636; (c) Y.-Q. Hu, M.-H. Zeng, K. Zhang, S. Hu, F.-F. Zhou and M. Kurmoo, *J. Am. Chem. Soc.*, 2013, **135**, 7901; (d) K. Zhang, M. Kurmoo, L.-Q. Wei and M.-H. Zeng, *Sci. Rep.* 2013, **3**, 2516; (e) Z. Yin, Q.-X. Wang and M.-H. Zeng, *J. Am. Chem. Soc.*, 2012, **134**, 4857; (f) M.-H. Zeng, Q.-X. Wang, Y.-X. Tan, S. Hu, H.-X. Zhao, L.-S. Long and M. Kurmoo, *J. Am. Chem. Soc.*, 2010, **132**, 2561.

11 (a) X. Lopez and J. M. Poblet, *Inorg. Chem.*, 2004, **43**, 6863. (b) M.-M. Rohmer and M. Bénard, *Chem. Soc. Rev.*, 2001, **30**, 340; (c) K. Okamoto, S. Uchida, T. Ito, N. Mizuno, *J. Am. Chem. Soc.*, 2007, **129**, 7378; (d) P. Mothé-Esteves, M. M. Pereira, J. Arichi, and B. Louis, *Cryst. Growth Des.*, 2010, **10**, 371.

12 (a) P.-Q. Zheng, Y.-P. Ren, L.-S. Long, R.-B. Huang and L.-S. Zheng, *Inorg. Chem.*, 2005, **44**, 1190; (b) I. V. Kozhevnikov, *Chem. Rev.*,1998, **98**, 171; (c) C. L. Hill and C. M. Prosser-Mc Cartha, *Coord. Chem. Rev.*, 1995, **143**, 407; (d) T. Okuhara, N. Mizuno and M. Misono, *Appl. Catal. A*, 2001, **222**, 63.

13 (a) K. Uehara, H. Nakao, R. Kawamoto, S. Hikichi and N. Mizuno, *Inorg. Chem.*, 2006, **45**, 9448; (b) Y.-G. Li, L.-M. Dai, Y.-H. Wang, X.-L. Wang, E.-B. Wang, Z.-M. Su and L. Xu, *Chem. Commun.*, 2007, 2593; (c) N. Mizuno and M. Misono, *Chem. Rev.*, 1998, **98**, 199.

14 One-pot hydrothermal syntheses of **1–3**: a mixture of CuO (0.081 g, 1 mmol), H_2MoO_4 (0.81 g, 5 mmol), L' (0.83 g, 10 mmol), L" (3.59 g, 30 mmol), hydrofluoric acid (40%, 7 mL) and water (10 mL) was stirred for about 6 h at room temperature, sealed in a 30-mL Teflon-lined stainless steel autoclave, and heated at 200°C for 3 days, then slowly cooled to room temperature at a rate of 5°C per hour. The resultant system was filtrated and the filtrate was kept to unchanged for vaporization for a few weeks. Finally, green crystals of **1** suitable for single-crystal X-ray diffraction analysis were first collected from the system after a week, then colorless crystals of **2** and **3** were obtained after two weeks and four weeks, respectively. For **1**, yield: *ca.* 50% based on CuO. Elemental anal (%). Calcd for $C_{32}H_{48}Cu_2Mo_8N_{16}O_{26}$: C, 19.54; N, 11.39; H, 2.46. Found: C, 19.64; N, 11.27; H, 2.54. ESI-MS (CH_3CN): m/z = 296 $[Mo_8O_{26}]^{4-}$. FTIR data (KBr, cm^{-1}): 2993 (w), 2557 (w), 2306 (s), 1879 (vs), 1775 (s), 1573 (w), 1265 (w), 1209 (w), 926 (w), 918 (w), 858 (s), 836 (s), 773 (w), 732 (w), 580 (w), 467 (w). For **2**, yield: *ca*. 40% based on H_2MoO_4. Elemental anal (%). Calcd for $C_{54}H_{59}Mo_{12}N_{27}O_{45}Si$: C, 21.72; N, 12.67; H, 1.99. Found: C, 21.66; N, 12.73; H, 2.07. ESI-MS (CH_3CN): m/z = 455 $[SiMo_{12}O_{40}]^{4-}$. FTIR data (KBr, cm^{-1}): 3719 (s), 2993 (w), 2541 (w), 2315 (w), 2202 (w), 1847 (s), 1782 (s), 1564 (w), 1297 (w), 1248 (w), 1209 (w), 932 (s), 887 (w), 839 (vs), 717 (w), 675 (w), 587 (w), 416 (w). For **3**, yield: *ca.* 20% based on H_2MoO_4. Elemental anal (%). Calcd for $C_{24}H_{28}Mo_{12}N_{12}O_{42}Si$: C, 12.34; N, 7.21; H, 1.21. Found: C, 12.38; N, 7.26; H, 1.24. Elemental analysis (%): Found: C, 12.38; N, 7.26; H, 1.24; Calc. for $C_{24}H_{28}Mo_{12}N_{12}O_{42}Si$: C, 12.34; N, 7.21; H, 1.21. ESI-MS (CH_3CN): m/z = 455 $[SiMo_{12}O_{40}]^{4-}$. FTIR data (KBr, cm^{-1}): 3751 (s), 2998 (w), 2557 (w), 2332 (vs), 2202 (w), 2072 (w), 1886 (vs), 1775 (s), 1573 (w), 1346 (w), 1274 (w), 1216 (w), 1154 (w), 926 (s), 893 (w), 838 (vs), 692 (w), 418 (w). Note that the Si atoms of **2** and **3** are from SiO_2 of the reaction glass vessel, which is dissolved by hydrofluoric acid.

15 Crystal data: For **1**, $C_{32}H_{48}Cu_2Mo_8N_{16}O_{26}$, M_r = 983.73, monoclinic, space group $P2_1/c$, a = 13.1126(15) Å, b = 16.1764(19) Å, c = 17.1279(15) Å, β = 123.896(6)°, V = 3015.6(6) Å^3, Z = 4, D_{calcd} = 2.167 g·cm^{-3}, μ = 2.382 mm^{-1}, $F(000)$ = 1908, GOF = 1.003, R_1 = 0.0573, wR_2 = 0.1441. A total of 15868 reflections were collected, of which 4529 (R_{int} = 0.1043) were unique. For **2**, $C_{54}H_{59}Mo_{12}N_{27}O_{45}Si$, M_r = 2985.65, monoclinic, space group $C2/m$, a = 23.3171(13) Å, b = 15.7546(9) Å, c = 12.0657(7) Å, β = 94.9490(10)°, V = 4415.8(4) Å^3, Z = 2, D_{calcd} = 2.245 g·cm^{-3}, μ = 1.765 mm^{-1}, $F(000)$ = 2900, GOF = 1.061, R_1 = 0.0514, wR_2 = 0.1479. A total of 16040 reflections were collected, of which 5149 (R_{int} = 0.0240) were unique. For **3**, $C_{24}H_{28}Mo_{12}N_{12}O_{42}Si$, M_r = 2335.95, triclinic, space group P-1, a = 11.6044(4) Å, b = 13.1169(4) Å, c = 20.4496(9) Å, V = 2779.28(18) Å^3, Z = 2, D_{calcd} = 2.791 g·cm^{-3}, μ = 2.749 mm^{-1}, $F(000)$ = 2220, GOF = 1.037, R_1 = 0.0382, wR_2 = 0.0825. A total of 53969 reflections were collected, of which 14351 (R_{int} = 0.0418) were unique. Intensity data were collected on a Bruker SMART CCD diffractometer equipped with a graphite-monochromated Mo K_α radiation (λ = 0.71073 Å) at 293(2) K using the ω-2θ scan technique. The structures were solved by direct methods and refined by full-matrix least-squares fitting on F^2 by SHELXTL-97. All nonhydrogen atoms were located from the initial solution and refined with anisotropic thermal parameters.

16 (a) W. A. Neiwert, J. J. Cowan, K. I. Hardcastle, C. L. Hill and I. A. Weinstock, *Inorg. Chem*., 2002, **41**, 6950; (b) X. Lopez, J. M. Maestre, C. Bo, J.-M. Poblet, *J. Am. Chem. Soc.*, 2001, **123**, 9571

17 (a) R. Hofhann and M. W. J. Lipscomb, *Chem. Phys*., 1962, **3**, 3179; (b) S.-H. Wangt and S. A. Jansen, *Chem. Mater.*, 1994, **6**, 2130; (c) R. Hoffmann, *J. Am. Chem. Soc*., 1978, **100**, 3686.

18 (a) Z.-L. Lang, W. Guan, Z.-J. Wu, L.-K. Yan and Z.-M. Su, *Comput. Theore. Chem*., 2012, **999**, 66; (b) W. G. Klemperer and W. Shum, *J. Am. Chem. Soc*., 1976, **98**, 8291; (c) L. Vilà-Nadal, A. Rodríguez-Fortea, L. K. Yan, E. F. Wilson, L. Cronin and J. M. Poblet, *Angew. Chem. Int. Ed*., 2009, **48**, 5452.

19 (a) K. Morokuma, *J. Chem. Phys.*, 1971, **55**, 1236; (b) T. Ziegler and A. Rauk, *Inorg. Chem*., 1979, **18**, 1558; (c) S. I. Gorelsky, S. Ghosh and E. I. Solomon, *J. Am. Chem. Soc.*, 2006, **128** (1), 278; (d) S. Ghosh, S. I. Gorelsky, P. Chen, I. Cabrito, J. J. G. Moura, I. Moura and E. I. Solomon, *J. Am. Chem. Soc*., 2003, **125**, 15708; (e) S. I. Gorelsky and E. I. Solomon, *Theor. Chem. Account*, 2008, **119**, 57.

20 Calculation details: The input data of $[Mo_8O_{26}]^{4-}$ anion and its $[MoO_4]^{2-}$ and $[Mo_6O_{18}]$ fragments in **1**, and $[SiMo_{12}O_{40}]^{4-}$ anion and its $[SiO_4]^{4-}$, $[Mo_{12}O_{36}]$, $[Mo_3O_9]$, and $[Mo_6O_{18}]$ fragments in **2** and **3**, are from the same crystal data, and are selected for respective electronic structure calculations based on extended Hückel theory method, and the default parameters of the employed Gaussian98 software. These calculated results are further analysed and compared to each other so as to understand the orbital interactions, charge transfer, electronic polarization between fragments employed the AOMix program. The solvent effect and basis set are not needed for considering in the extended Hückel theory calculations.

Graphical Abstract

Synthesis, Structures and Theoretical Investigation of Three Polyoxomolybdate-based Compounds: Self-assembling, Fragment Analysis, Orbital Interaction, and Formation Mechanism

Yi-Ping Tong, Guo-Tian Luo, Jin Zhen, You Shen, and Yan-Wen Lin

Three Mo_8- and Mo_{12}-based compounds, containing $[Mo_8O_{26}]^{4-}$ and $[(SiO_4)(Mo_{12}O_{36})]^{4-}$ polyoxoanions, were synthesized from a solution system. It is very rare and very interesting in POM synthetic chemistry. Both fragment analysis and orbital interaction analysis were employed to explain the formation and self-assembling mechanism of the polyoxoanions.